Journal of Cellular Biochemistry 98:519–537 (2006)

Purification and Characterization of a Novel Mammalian Endoribonuclease

Kirk Bergstrom, Joel C. Urquhart, Alaeddin Tafech, Erin Doyle, and Chow H. Lee*

Chemistry Program, University of Northern British Columbia, 3333 University Way, Prince George, BC V2N 4Z9, Canada

Abstract Endonuclease-mediated mRNA decay appears to be a common mode of mRNA degradation in mammalian cells, but yet only a few mRNA endonucleases have been described. Here, we report the existence of a second mammalian endonuclease that is capable of cleaving c-*myc* mRNA within the coding region in vitro. This study describes the partial purification and biochemical characterization of this enzyme. Five major proteins of ~10–35 kDa size co-purified with the endonuclease activity, a finding supported by gel filtration and glycerol gradient centrifugation analysis. The enzyme is an RNA-specific endonuclease that degrades single-stranded RNA, but not double-stranded RNA, DNA or DNA–RNA duplexes. It preferentially cleaves RNA in between the pyrimidine and purine dinucleotides UA, UG, and CA, at the coding region determinant (CRD) of c-*myc* RNA. The enzyme generates products with a 3′hydroxyl group, and it appears to be a protein-only endonuclease. It does not possess RNase A-like activity. The enzyme is capable of cleaving RNAs other than c-*myc* CRD RNA in vitro. It is Mg^{2+}-independent and is resistant to EDTA. The endonuclease is inactivated at and above 70°C. These properties distinguished the enzyme from other previously described vertebrate endonucleases. J. Cell. Biochem. 98: 519–537, 2006. © 2005 Wiley-Liss, Inc.

Key words: c-*myc* mRNA; mammalian mRNA degradation; mammalian endoribonuclease

Steady-state levels of mRNAs can be influenced by the rate of precursor mRNA synthesis in the nucleus, nuclear RNA processing and export, and degradation of mature cytoplasmic mRNA. In recent years, there has been increasing evidence to indicate a critical role of mRNA degradation in the regulation of eukaryotic gene expression, under physiological and pathological conditions [Ross, 1995; Brewer, 2002; Dodson and Shapiro, 2002; Parker and Song, 2004]. For instance, when cultured cells were exposed to stress stimulus, mRNA stabilization and destabilization significantly influencedapproximately 53% of stress-regulated genes [Fan et al., 2002]. Similarly, hundreds of transcripts showed stimulus-dependent changes in mRNA decay upon T-cell activation in primary human T-lymphocytes [Raghavan et al., 2002]. Adding further excitement is the possible link between the basic mRNA decay machinery and an anti-viral defense mechanism, as in RNA interference [Carmell and Hannon, 2004; Parker and Song, 2004]. Interestingly, this link has recently been demonstrated in *Arabidopsis* [Gazzani et al., 2004].

Much of our understanding of the eukaryotic mRNA decay pathways and enzymes has come from studies in yeast [Parker and Song, 2004]. For instance, it is now known that deadenylation followed by decapping and 5′–3′ exoribonucleolytic decay is one major decay pathway in yeast [Parker and Song, 2004]. A second major decay pathway in yeast involves 3′–5′ exoribonucleolytic degradation by the exosomes following deadenylation [Parker and Song, 2004]. While endonucleolytic cleavage within the body of the mRNA does not appear to be a major mode of decay in yeast [Tharun and Parker, 1997], it

Abbreviations used: CRD, coding region determinant; RSW, ribosomal salt wash; UTR, untranslated region; MNase, micrococcal nuclease.

Grant sponsor: Natural Sciences & Engineering Research Council; Grant sponsor: Canadian Breast Cancer Foundation; Grant sponsor: Canadian Cancer Society.

*Correspondence to: Chow H. Lee, Chemistry Program, University of Northern BC, 3333 University Way, Prince George, BC V2N 4Z9, Canada. E-mail: leec@unbc.ca

Received 10 September 2005; Accepted 11 October 2005

DOI 10.1002/jcb.20726

© 2005 Wiley-Liss, Inc.

has been reported for a number of mRNAs in vertebrates [Dodson and Shapiro, 2002]. For example, endoribonucleases have been shown to be responsible for degradation of the human transferrin receptor [Binder et al., 1994], human insulin-like growth factor II [Van Dijk et al., 1998], human α-globin [Wang and Kiledjian, 2000], human β-globin [Stevens et al., 2002], human c-*myc* [Ioannidis et al., 1996; Lee et al., 1998; Tourriere et al., 2001], mouse [Tharun and Sirdeshmukh, 1995] and *Xenopus* albumin [Hanson and Schoenberg, 2001], *Xenopus* vitellogenin mRNA [Cunningham et al., 2001], and mRNAs containing premature termination codons in *Drosophila* [Gatfield and Izaurralde, 2004]. Due to technical limitations and the fact that endonucleases with similar catalytic mechanisms diverge widely at the amino acid sequence level [Dodson and Shapiro, 2002], only a handful of these enzymes have been identified and studied in vertebrates. Known members of this group include an estrogen-regulated polysomal endonuclease termed PMR1 that preferentially cleaves single-stranded RNA at UG sites [Chernokalskaya et al., 1998], G3BP, associated with the Ras GTPase-activating protein that cleaves between cytosine and adenine residues at 3′ UTR of c-*myc* mRNA [Tourriere et al., 2001], and an endonuclease called activator of RNA decay which has functional but not sequence homology to RNase E [Claverie-Martin et al., 1997].

c-*myc* mRNA is one of the mammalian mRNAs whose decay mechanism has been well-studied [Ross, 1995; Brewer, 2002]. By using cell-free mRNA decay assays as well as in vivo analysis, it has been demonstrated that c-*myc* mRNA can be degraded by two different pathways. One involves rapid removal of the poly(A) tail followed by 3′–5′ decay accomplished by a yet undefined 3′–5′ exoribonuclease(s) [Brewer, 1999, 2000]. The second mode of decay for c-*myc* mRNA involves an endonuclease whose activity was initially discovered using a polysome-based cell-free mRNA decay assay [Bernstein et al., 1992]. This endonuclease targets the C-terminal coding region of an endogenous polysome-associated c-*myc* mRNA referred to as the c-*myc* coding region determinant or CRD. Several studies have confirmed that the coding region of c-*myc* mRNA, including the CRD, is part of the major determinant of c-*myc* mRNA stability in cells [Wisdom and Lee, 1991; Bernstein et al., 1992; Herrick and Ross, 1994; Yielding and Lee, 1997]. The relationship of the endonuclease to the c-*myc* CRD and to c-*myc* mRNA stability is further supported by findings that c-*myc* mRNA can be degraded endonucleolytically in cells [Swartwout and Kinniburgh, 1989; Ioannidis et al., 1996; Hanson and Schoenberg, 2001].

A polysomal-associated enzyme that is capable of degrading the CRD of c-*myc* mRNA in vitro has been partially purified from rat liver [Lee et al., 1998]. This enzyme has properties resembling the polysomal c-*myc* endonuclease [Lee et al., 1998]. In an effort to further purify and identify this enzyme, we fortuitously discovered a second novel enzyme that is also capable of degrading the CRD of c-*myc* mRNA. In view of the significance of finding mammalian endonucleases involved in mRNA turnover and their possible link to RNA interference, and evidence for the role of endonuclease in governing c-*myc* mRNA abundance in cells, we have initiated further studies on the second novel enzyme. Here, we describe the partial purification and biochemical characterization of the second enzyme. We provide evidence that this enzyme has properties that distinguish it from other known vertebrate endonucleases.

MATERIALS AND METHODS

Materials

Frozen livers from male Sprague–Dawley rats purchased from Harlan Bioproducts (Madison, Wisconsin) were used for preparation of ribosomal salt wash and partially purified proteins described in this study. T4 polynucleotide kinase and ribonucleoside vanadyl complex were from New England Biolabs (Ontario, Canada). Alkaline phosphatase and RNase T1 were obtained from Roche Applied Sciences (Laval, Quebec). SP6 Megascript kits were purchased from Ambion (Austin, Texas). RNasin was purchased from Promega (Madison, WI) and [γ-^{32}P] ATP (3,000 Ci/mmol) was from Amersham Biosciences (Montreal, Quebec). All other chemicals were either purchased from VWR or Fisher Scientific (Ontario, Canada).

Preparation of Ribosomal Salt Wash

Frozen livers from male Sprague-Dawley rats were used for all protein purification experiments described in this study. All

procedures were performed on ice unless otherwise indicated. Frozen livers were homogenized in Buffer A (1 mM potassium acetate, 1.5 mM magnesium acetate, 2 mM DTT, 10% (v/v) glycerol, 0.1 mM EGTA, 10 mM Tris-Cl, pH 7.4) (1 ml Buffer A for every 0.4 g tissues) for 2–3 min using a Polytron. Subsequent steps for the preparation of liver polysomes and salt-eluted polysomal proteins designated as ribosomal salt wash (RSW) have been previously described [Lee et al., 1998]. Typically, between 50 and 75 mg of RSW proteins can be obtained from one liver weighing 175–200 g.

Preparation of Radiolabeled Nucleic Acids

The plasmid DNA, pUC19-CRD*myc*, used in this study was constructed by sub-cloning a PCR product corresponding to nucleotides 1705–1792 of human c-*myc* mRNA into *Bam*HI and *Eco*RI restriction sites of pUC19. The PCR product was generated using primers FUP (5′-CTCGGATCCATTTAGGTGACACTATAGACCAGATCCCGGAGTTGG, corresponding to nts 1705–1722 of human c-*myc* mRNA and containing a *Bam*HI restriction site as indicated by underlined nucleotides) and RUP (5′-CTCGAATTCGCTTGGACGGACAGGATG, corresponding to nt 1775–1792 of human c-*myc* mRNA and contained a *Eco*RI restriction site as indicated by underlined nucleotides), using the human c-*myc* cDNA as template. The RNA corresponding to c-*myc* nts 1705–1792 is referred throughout this article as CRD RNA. The 5′-^{32}P-end labeling of CRD RNA was used as the substrate for purifying and characterizing liver endonucleases. Unlabeled CRD RNA was synthesized by linearizing pUC19-CRD*myc* with *Eco*RI and transcribing the DNA with SP6 polymerase using SP6 Megascript kits (Ambion, TX). The plasmid DNA, pGEM4Z-myc 1705–1886 was made by sub-cloning a PCR product corresponding to nucleotides 1705–1886 of human c-*myc* mRNA into *Bam*HI and *Hind*III restriction sites of pGEM4Z. The PCR product was generated using primers F1705–1722 (5′CTCGGATCCACCAGATCCCGCACCAGATCCCGGAGTTGG) and R1869–1886 (5′CGACAAGCTTCGCACAAGAGTTCCGACAAGAGTTCCGTAG), using human c-*myc* cDNA as template. Unlabeled sense RNA corresponding to nts 1705–1886 was made by linearizing the DNA with *Hind*III and transcribing the DNA with SP6 polymerase. To make anti-sense RNA corresponding to nts 1705–1886, the DNA was linearized with *Eco*RI and transcribed with T7 RNA polymerase.

For 5′-^{32}P-end labeling of RNA, 5 μg of in vitro transcribed RNA was first dephosphorylated with 10 units of alkaline phosphatase for 30 min at 37°C in a 100-μl reaction according to the manufacturer's instructions. Dephosphorylated RNA was purified by phenol/chloroform extraction and ethanol precipitation. 2.5 μg of dephosphorylated RNA was incubated in a 25-μl reaction with 30–50 μCi of [γ-^{32}P] ATP at 37°C for 1 h with 40–50 U of T4 polynucleotide kinase. The entire sample was then run on a 6% polyacrylamide/7 M urea gel and the band containing 5′-labeled ^{32}P-RNA was sliced out and eluted with elution buffer (0.5 M ammonium acetate, 1 mM EDTA, 0.2% SDS) at 37°C for 6 h. The purified radiolabeled RNA was then concentrated by ethanol precipitation.

Oligonucleotides myc1705–1792 and myc 1792–1705 were purchased from QIAGEN (Alameda, CA). 5′-^{32}P-end labeling of DNA was essentially as described above for 5′-end labeling for RNA.

For preparation of double-stranded RNA or DNA, 1 ng of 5′-labeled ^{32}P-RNA or DNA was first heated to 80–90°C for 5 min with 5 ng of complementary DNA or RNA strand in 40 mM PIPES, pH 6.4, 400 mM NaCl, 1 mM EDTA, and 80% formamide. The nucleic acids were then allowed to hybridize overnight at 52°C, followed by ethanol precipitation. The double-stranded RNA, DNA, or RNA–DNA duplexes were then purified from a 10% non-denaturing polyacrylamide gel.

In Vitro Assay for Endonuclease Activity

The pH of all buffers for experiments described here was determined at room temperature. The standard 20–25-μl reaction mixture used for this assay included 2 mM DTT, 1.0 U of RNasin, 2 mM magnesium acetate, 50 mM potassium acetate, 0.1 mM spermidine, 1 ng of 5′-end-labeled ^{32}P-RNA (approximately 5×10^4 cpm), and 10 mM Tris-HCl, pH 7.4. Reactions were incubated for 5 min at 37°C unless otherwise indicated, placed in liquid nitrogen, and then at 80–90°C to inactivate enzyme activities. Five μl of loading dye (9 M urea, 0.2% xylene cyanol, 0.2% bromophenol blue) were added to 5 μl of reaction samples, and then subjected to electrophoresis for 75 min in a 6% polyacrylamide, 7 M urea gel. Gels were fixed in 10% acetic acid, 10% methanol for 15 min,

and then dried and exposed to a PhosphorImager screen (Cyclone PhosphorImager).

Partial Purification of Liver Polysomal Endoribonuclease

The pH of approximately 28 g of RSW proteins was adjusted to 5.0 using HCl, and then spun at 18,000*g* for 20 min at 4°C to pellet precipitated proteins. The supernatant was recovered and the pH was adjusted to 7.0 using sodium hydroxide. Approximately 1.8 g of pH 7.0-adjusted RSW proteins were loaded at a flow rate of 1.8 ml/min on 5 × 48 cm phosphocellulose column (Sigma) equilibrated with 0.05 M KCl in 25 mM potassium phosphate, pH 6.0 (Buffer B). The column was washed with three volumes of Buffer B, or until the absorbance at 280 nm (A_{280}) had returned to baseline. The column wash was collected and stored at 4°C. Bound proteins were eluted with a linear gradient from 0.05 to 1.0 M KCl in three volumes of Buffer B. 30 ml fractions were collected and 1 μl aliquots were taken from every fourth fraction for endonuclease activity assay as described above. For reasons, which are unclear to us, weak endonuclease activity was detected in the column wash. Therefore, any column wash containing endonuclease activity was reloaded directly onto the phosphocellulose column in a separate run. Twelve separate phosphocellulose columns were conducted, and each column yielded highly reproducible results. Fractions containing at least 60 % of maximal endonuclease activity from each column were pooled.

The pooled phosphocellulose fractions were diluted to approximately 0.1 M KCl by the addition of three volumes of 0.05 M KCl in 50 mM triethanolamine, pH 7.4 (Buffer C). It was then loaded at a flow rate of 1 ml/min onto 2.5 × 16 cm Reactive blue-4 column (Sigma) equilibrated with Buffer C. The column was washed with five volumes of Buffer C, or until A_{280} had returned to zero. Bound proteins were eluted with a linear gradient from 0.05 to 1.0 M KCl in five volumes of Buffer C. 3.0 ml fractions were collected and assayed for presence of endonuclease activity, and active fractions containing 60 % of maximal endonuclease activity were pooled. Fourteen separate 2.5 × 16 cm Reactive blue 4 columns were conducted, and each produced similar results.

To dilute the pooled Reactive blue-4 sample to 0.1 M KCl, four volumes of Buffer C were added. It was then loaded at a flow rate of 1 ml/min onto a 2.5 × 16 cm Reactive green-19 column (Sigma) and equilibrated with Buffer C. The column was washed with Buffer C, and bound proteins were eluted with a linear gradient from 0.05 M KCl to 1.0 M KCl in five volumes of the same buffer. Two milliliter fractions collected were assayed for endonuclease activity. Two separate Reactive green-19 columns were conducted, and each yielded similar results. Fractions containing at least 60% of maximal endonuclease activity were pooled.

To dilute the pooled Reactive green-19 samples to approximately 0.1 M KCl, seven volumes of Buffer C were added. It was then loaded at a flow rate of 0.75 ml/min onto a 2.5 × 14 cm Affi-Gel Heparin gel column (Bio-Rad) and equilibrated with Buffer C. The column was washed with five volumes of Buffer C, and bound proteins were eluted with a linear gradient from 0.05 to 1.0 M KCl in five volumes of the same buffer. 1.5 ml fractions were collected and assayed for endonuclease activity. Fractions containing at least 70% of maximal endonuclease activity were pooled. Two separate Affi-Gel Heparin gel columns were conducted, and each produced similar results.

To dilute the pooled Affi-Gel Heparin gel fractions to approximately 0.1 M KCl, five volumes of Buffer C were added. The diluted pooled fractions were applied at a flow-rate of 0.75 ml/min onto a 5.0 ml pre-packed heparin-Sepharose column (Amersham Bioscience, Quebec) and equilibrated with Buffer C. The column was washed with 10 volumes of Buffer C, and bound proteins were eluted with a linear gradient from 0.05 to 1.0 M KCl in five volumes of the same buffer. 0.25 ml fractions collected were assayed immediately for endonuclease activity. Fractions containing at least 70% of maximal endonuclease activity were pooled. Two separate heparin-Sepharose columns were performed, and each yielded similar results.

One unit of partially purified post-heparin Sepharose endonuclease was used for most experiments described throughout this study unless otherwise indicated, and was defined as the amount of enzyme required to cleave ~30% of the input RNA substrate into decay product in a 5-min reaction at 37°C.

Glycerol Gradient Centrifugation of Partially Purified Enzyme

Partially purified enzyme (0.2 ml of post-heparin-sepharose sample) was layered onto a

10–70% (v/v) glycerol gradient (3.85 ml, 11 × 60-mm tubes) made in 0.25 M KCl, 0.1 mM EDTA, 50 mM Tris-HCl, pH 7.4, and was centrifuged for 18 h, 4°C, 200,000*g* (44,100 rpm) in a Beckman SW 60 rotor. Fractions of 100 μl (for protein standards) or 200 μl (for RSW and post-heparin) were collected manually from the top. Four microliters of each fraction (for RSW and post-heparin) were assayed for endonuclease activity. A separate 10–70% glycerol gradient was centrifuged in the same manner and contained the following proteins as molecular mass standards (Amersham Biosciences, Quebec): myosin (205 kDa), β-galactosidase (116 kDa), phosphorylase b (97 kDa), transferrin (80 kDa), albumin (66 kDa), glutamate dehydrogenase (55 kDa), ovalbumin (45 kDa), carbonic anhydrase (30 kDa), trypsin inhibitor (21 kDa), lysozyme (14 kDa), and aprotinin (6.5 kDa). The protein standards were identified by silver staining of SDS–PAGE.

Gel Filtration Chromatography of Partially Purified Enzyme

Partially purified enzyme from post-phosphocellulose column (3 ml; 1 mg of protein) was first dialyzed overnight in 0.15 M KCl, 50 mM triethanolamine, pH 7.4 at 4°C using PIERCE Slide-A-Lyzer dialysis cassette. Dialyzed enzyme was then chromatographed at room temperature on a Sephacryl S-100 (Amersham) column equilibrated with 0.15 M KCl, 50 mM triethanolamine, pH 7.4. The column was run at 0.5 ml/min, and 0.4-ml fractions were collected. A 4-μl aliquot of fractions was assayed for endonuclease activity. The column was calibrated with myoglobin (17 kDa), ovalbumin (45 kDa), and SIGMA molecular weight markers: Blue dextran 2000 (2,000 kDa), β-amylase (200 kDa), alcohol dehydrogenase (150 kDa), bovine serum albumin (66 kDa), carbonic anhydrase (29 kDa), and cytochrome-*c* (12.4 kDa). The elution of these proteins was determined by absorbance at 280 nm and further confirmed by silver stained SDS–PAGE.

RESULTS

Partial Purification of the Liver Endonuclease

The significance of identifying and studying endonucleases for c-*myc* mRNA stems from the first observation in a cell-free mRNA decay assay, where Ross and co-workers discovered the existence of a polysomal c-*myc* mRNA-degrading endonuclease [Bernstein et al., 1992]. Under reaction conditions where RNA-binding proteins were thought to be titrated, polysome-associated c-*myc* mRNA was cleaved endonucleolytically in the CRD. The importance of endonuclease(s) that cleave CRD was further highlighted by the findings that the CRD is a major determinant of c-*myc* mRNA expression and stability in vivo [Wisdom and Lee, 1991; Herrick and Ross, 1994; Yielding and Lee, 1997], and the fact that c-*myc* mRNA is cleaved endonucleolytically in some cells [Swartwout and Kinniburgh, 1989; Ioannidis et al., 1996; Hanson and Schoenberg, 2001].

There are three reasons for using high salt ribosomal salt washes (RSW) as our choice of starting material. (i) c-*myc* mRNA abundance was regulated post-transcriptionally in rodent liver during fetal development and liver regeneration [Steer, 1996], and that the c-*myc* coding region is required for the regulation [Morello et al., 1990; Pistoi et al., 1996]. (ii) Liver provides an abundant source of starting material for purification and was readily accessible. (iii) Crude liver extract was found to contain endonuclease(s) that cleave the CRD of c-*myc* mRNA at regions that corresponded to the sites cleaved by the polysome-associated c-*myc*-degrading enzyme [Bernstein et al., 1992].

The first step in the purification was the isolation of proteins in RSW from rat liver. This step was achieved by the removal of nuclei and the bulk of cytoplasmic organelles, thus generating crude polysomal extracts. Proteins that were eluted with high salt from the crude polysomes designated as RSW were used as the starting material. The enzyme was purified through five column chromatographic steps and one non-chromatographic approach. The purification scheme is outlined in Figure 1A. We first subjected the RSW to the non-chromatographic pH-precipitation step, as it increased the purification by approximately fourfold (Table I). Following the adjustment of pH back to 7, the proteins in the supernatant were bound to phosphocellulose and eluted with an increasing KCl gradient up to 1.0 M KCl. Proteins in active fractions eluted at ~0.55 M KCl were pooled, diluted, and bound to a reactive blue-4 column. Proteins in active fractions eluted at ~0.35 M KCl from reactive blue-4 column were pooled, diluted, and bound to reactive green-19 column. Proteins that eluted at ~0.6 M KCl which contained endonuclease activity, were

TABLE I. Partial Purification of Rat Liver Endonuclease

Step	Total protein (mg)	Volume (ml)	Activity (Units)	Specific activity (Units/mg)	Yield (%)	Purification (-Fold)
Ribosomal salt wash	28,922	8,799	3.2×10^7	1,108	100	1
PH precipitation	20,364	8,799	9.7×10^7	4,753	>100	4.3
Phosphocellulose	667	7,133	1.6×10^7	23,733	49	21
Reactive blue-4	3.7	491	1.1×10^6	287,719	3.3	260
Reactive green-19	0.36	102	2.6×10^5	710,753	0.8	642
Affigel	0.11	46	9.4×10^4	926,764	0.3	837

Endonuclease activity was determined in the linear range at each step of the purification except after the heparin-Sepharose column. One unit of endonuclease was defined as the amount of enzyme required to cleave 30% of the input RNA substrate into decay products in a 5-min reaction at 37°C.

pooled, diluted, and bound to an Affi-gel column. Active fractions eluted at ~0.5 M KCl from the Affi-gel column were also pooled and diluted. Specific activity of the endonuclease was measured at each purification step as shown in Table I. The table also shows that the endonuclease can be purified up to about 840-fold on the fourth chromatographic step, the Affi-gel column. The degree of purification fold after the final chromatography step, the heparin-Sepharose column, could not be determined because the amount of protein recovered was too small. This data, is therefore, not included in Table I. Pooled active fractions from each purification step, from pH precipitation to Affi-gel column, were resolved on SDS–PAGE and visualized by silver staining as shown in Figure 1B.

Proteins from pooled and diluted active fractions from Affi-gel were bound to the last purification column heparin-sepharose, and eluted with an increasing KCl gradient from 0.05 to 1.0 M KCl. Aliquots from the active and surrounding fractions from heparin-sepharose column were resolved on a SDS–PAGE and visualized by silver staining shown in the top panel of Figure 1C. The assay for endonucleolytic activity for the corresponding fractions is shown at the bottom panel of Figure 1C. The endonuclease activity recovered from heparin-sepharose column contained only several observable proteins (see fraction 86 on top panel of Fig. 1C). A comparison of enzyme activity, as indicated by intensity of degradation products (filled arrow, bottom panel), with the protein elution profile of fractions 82–102 showed that there are five bands, one at ~35 kDa (shown by arrow) and four at ~10–25 kDa (shown by arrow) on SDS–PAGE, which corresponded to the endonuclease activity. Closer examination shows that the lower molecular weight bands (~10–25 kDa) correlate better with the endonuclease activity. To help provide further support in determining the sizes of proteins, which contribute to the endonuclease activity, glycerol gradient centrifugation and gel filtration experiments were performed. A glycerol gradient centrifugation experiment using the partially purified enzyme shown in Figure 2A, indicated that the endonuclease activity peaks at ~1.0 ml from top of the tube. This corresponded with the sedimentation of protein at ~34 kDa. Gel filtration chromatography was performed under non-denaturing conditions. As shown in Figure 2B, two endonuclease activities were visible, one significantly more prominent at elution volume of ~48 ml which corresponded to ~35 kDa protein, and the other much weaker activity eluted at volume of ~61.2 ml which corresponded to ~13 kDa protein. In summary, our data showed that five major proteins (~10–35 kDa sizes) were co-purified with the endonuclease activity (Fig. 1C). Glycerol gradient centrifugation and gel filtration experiments provided further evidence in support of the proposal that either one or a combination of some of the proteins contributes to the endonuclease activity. It is also possible that the smaller polypeptides are the degradation products or modified proteins of the larger ~35 kDa proteins, or that the 35 kDa protein is a dimer of two of the smaller polypeptides.

In contrast to a previously described endonuclease [Lee et al., 1998], the endonuclease described in this article was stable and could be purified without the addition of a carrier

protein. As a result, it was possible to determine the extent of purification of the endonuclease, as shown in Table I.

CRD Cleavage Sites Generated by the Endonuclease

To precisely map the cleavage sites generated by the endonuclease, we ran c-*myc* 5′-CRD ^{32}P-RNA substrates that had been treated with the enzyme along side with c-*myc* 5′-CRD ^{32}P-RNAs that had been subjected to a partial RNase T1 digestion and alkaline hydrolysis (Fig. 3A). Under partial digestion condition, RNase T1 preferentially cleaves after single-stranded guanosine (G) residues in regions that are accessible. Fragments generated by partial RNase T1 digest, as shown by left hand pointed arrows in Figure 3A, were successfully identified, and G sites were mapped accordingly. Using these mapped G sites and the alkaline ladder, the major cleavage sites generated by the endonuclease were identified as shown in

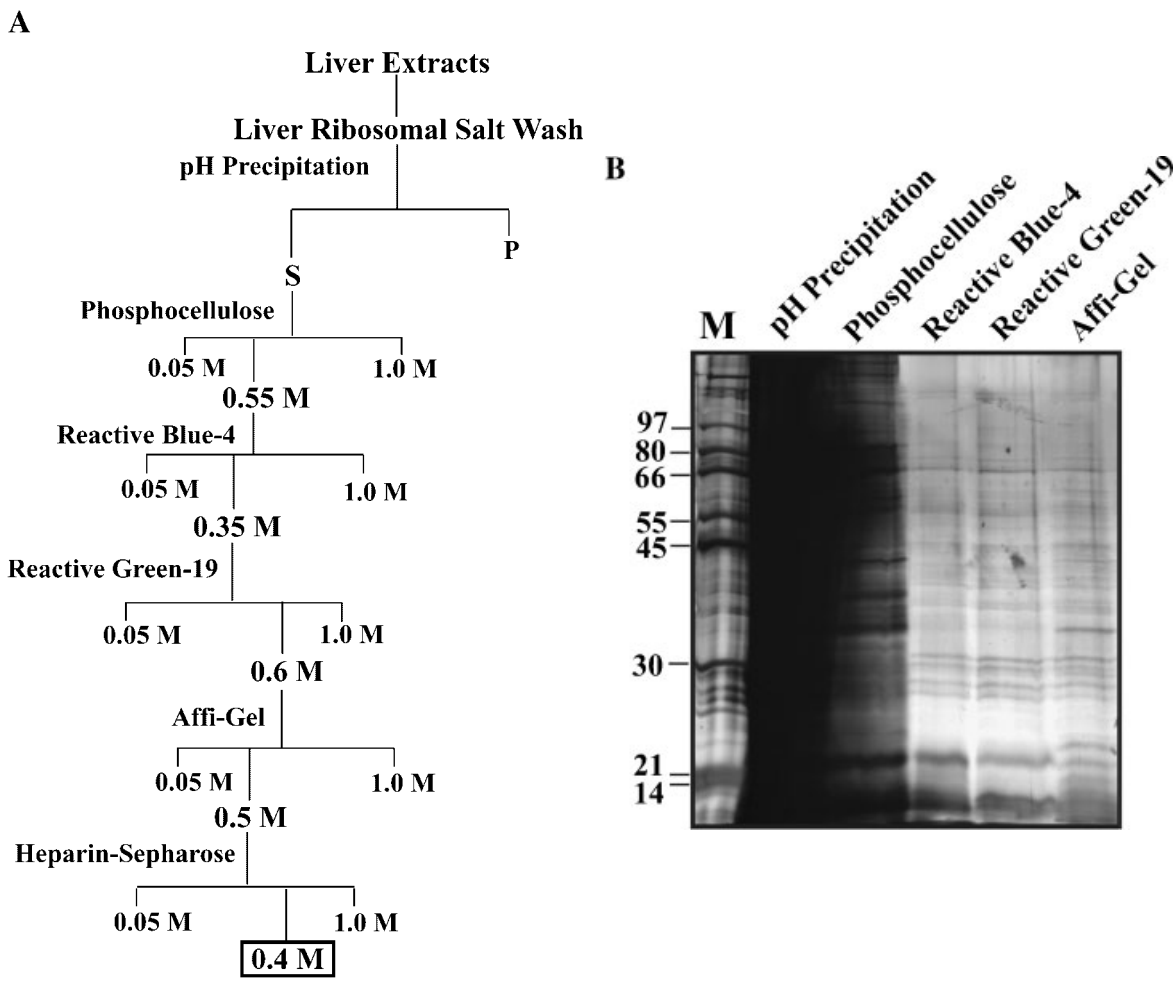

Fig. 1. Partial purification of the endonuclease from rat liver. **A**: The purification scheme is outlined with the columns and fractionation listed on the **left**. Horizontal lines indicate an elution gradient. S indicates the supernatant and P is the precipitate. The fractions containing enzyme activity are in bold type. The final gradient resulting in the purification of the endonuclease is boxed at the bottom. **B**: Thousand units of endonuclease from each activity peak of each column except heparin-Sepharose were separated by SDS–PAGE and visualized by silver staining. Protein size markers (M) shown on the left are in kDa. **C**: Silver-stained SDS–PAGE from fractions 70–102 of heparin-Sepharose gradient eluted with increasing concentration of KCl ranging from 0.05 to 1.0 M is shown in the **top** panel. The candidate bands (~35 and ~10–25 kDa) corresponding to the endonuclease activity are indicated by arrows on the **right**. The **bottom** panel is result of an autoradiograph for assaying the presence of endonuclease activity in post-heparin-Sepharose fractions (fractions 60–137) using 5′^{32}P-labeled CRD c-*myc* RNA as substrate. Fractions 70–102 correspond to the silver-stained SDS–PAGE in the top panel. The control lane at the bottom panel is partially purified post-Affigel enzyme. Unfilled arrow on the right indicates the undigested substrate RNA; filled arrow indicates endonucleolytic decay products generated by the endonuclease. Marker, indicated by numbers on the left, is 5′-labeled ^{32}P-pBR322 DNA cleaved with *Hae*II.

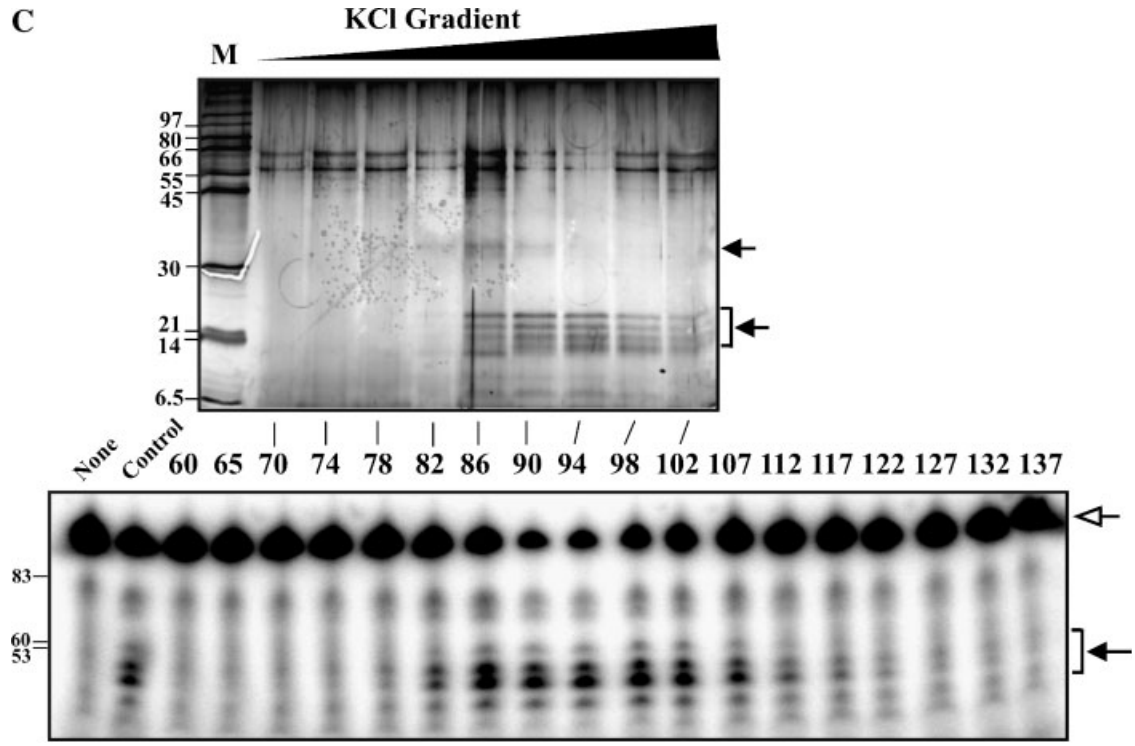

Fig. 1. (*Continued*)

Figure 3B. Major cleavages sites generated by the endonuclease on nts 1705–1792 c-*myc* CRD (left panel in Fig. 3A), shown by solid lines, were at CA (nts 1727, 1742, 1768, 1771, 1775), UA (nts 1747, 1751, 1757, 1773) and UG (nts 1720, 1730). To further address the enzyme's specificity for those cleavage sites and to further identify other endonucleolytic cleavage sites on the CRD, we challenged the enzyme with nts 1705–1886 of c-*myc* CRD RNA. As shown in the right panel of Figure 3A, the same cleavage sites, indicated by asterisks (nts 1742, 1747, 1751, and 1757), were generated by the endonuclease on both 1705–1792 and 1705–1886 RNA substrates. Cleavage sites at nts 1766, 1768, 1771, 1773, and 1775 generated on substrate 1705–1886 CRD RNA (right panel in Fig. 3A), were also generated on the substrate 1705–1792 CRD RNA (left panel in Fig. 3A). Additionally, the right panel in Figure 3A shows that the endonuclease cleaved at CA sites at nts 1788, 1792, 1800, and 1808, further confirming that the enzyme preferentially cleaves some CA sites. Figure 3B shows the summary of all the sites in CRD that are cleaved by the endonuclease.

The above approach was also used to map the cleavage sites generated by the previously described liver endonuclease [Lee et al., 1998] (data not shown). The summary of these sites are shown as broken lines above sequences in Figure 3B.

The Enzyme is an Endonuclease

To demonstrate that the enzyme is truly an endonuclease, it was incubated with 88-nt CRD RNA (nts 1705–1792) that was ^{32}P-labeled at either the 5′ or 3′ terminus. The 5′-labeled substrate was cleaved by the endonuclease to generate four major distinct fragments, which were easily observable on a 12% polyacrylamide gel. These four fragments were identified as nts 1742, 1747, 1751, and 1757, numbered 1–4 as shown in Figure 4 (lanes 4 and 5). The 3′-labeled substrate was also cleaved by the enzyme to generate four distinct fragments which were observable on a 12% denaturing gel (lanes 9 and 10 in Fig. 4). Close examination of these fragments (bands 1–4) (lanes 9 and 10) showed that they corresponded precisely to the four 5′-labeled degradation products (bands 1–4) (lanes 4 and 5) generated by the enzyme. These

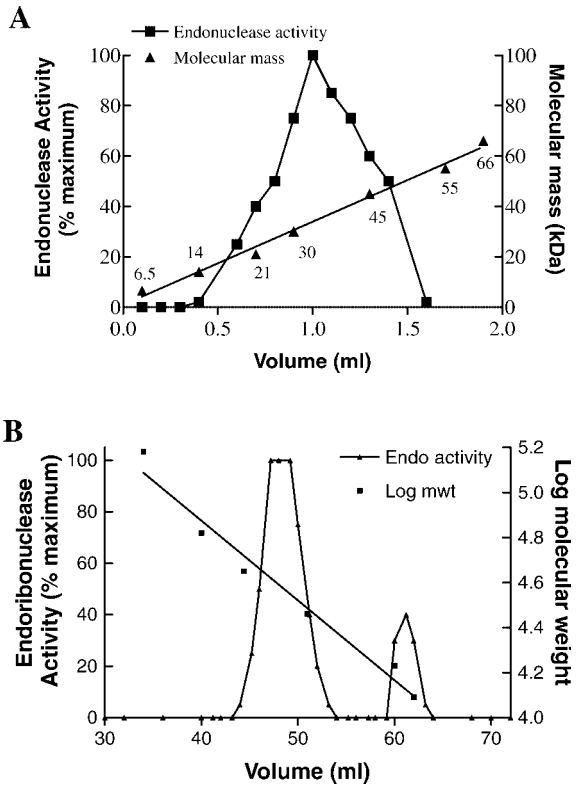

Fig. 2. Analysis of the partially purified endonuclease by glycerol gradient centrifugation and gel filtration. **A**: Partially purified enzyme from post-heparin Sepharose (0.2 ml) was centrifuged in a 10–70% glycerol gradient and aliquot from each fraction was assayed for endonuclease activity as described in Materials and Methods. Endonuclease activity was expressed as percent of maximal endonucleolytic product generated. A parallel gradient containing molecular mass marker proteins were spun and an aliquot from fractions were run on a 12% SDS–PAGE gel and the location of protein standards were identified by silver staining. **B**: Gel filtration was calibrated with molecular weight markers before chromatography with 1 mg of partially purified endonuclease under native conditions. Endonuclease activity was expressed as percent of maximal endonucleolytic product generated. Volumes at which protein standards were eluted as determined by silver-stained SDS–PAGE, and at which endonuclease activities were assayed, are shown on the Y-axis.

results lead us to conclude that the enzyme is an endonuclease.

The Endonuclease is a Protein-Only Enzyme

Some well-established ribonucleases involved in RNA metabolism, such as RNase P [Gopalan et al., 2002] and RNase MRP [Xiao et al., 2002], are known to require an RNA cofactor for their activity. To address whether an RNA cofactor is required for activity by the endonuclease, the partially purified enzyme was treated with micrococcal nuclease as shown in the experiment described in Figure 5. Lane 3 shows that degradation of ^{32}P-CRD RNA by the partially purified endonuclease using the standard endonuclease assay. Addition of 17 mM EGTA further enhanced the enzyme activity (lane 4). This is consistent with our findings that the endonuclease activity was increased in the presence of EDTA (unpublished observation). Addition of 5×10^{-2} U of micrococcal nuclease, either alone (lane 5), or in the presence of the endonuclease (lane 7), resulted in complete digestion of ^{32}P-CRD RNA. This degradation was prevented by co-addition of 17 mM EGTA (lanes 6 and 8). In lane 9, three units of the endonuclease were first incubated with micrococcal nuclease. Seventeen millimolars of EGTA was then added to inactivate the micrococcal nuclease followed by incubation with ^{32}P-CRD RNA. Lane 10 is similar to lane 9, except that the endonuclease was incubated with water instead of micrococcal nuclease. Our results show the endonuclease remained active in the presence of EGTA, and that addition and pretreatment of micrococcal nuclease had no effect on the endonuclease activity. We conclude that the endonuclease does not require an RNA cofactor for activity and that catalytic RNA is not responsible for the nucleolytic activity observed in our assays.

The Enzyme Generates Product With 3′ Hydroxyl Group

In view of the fact that (i) a major pathway of mRNA degradation in bacteria involves endonucleolytic cleavage by RNase E followed by 3′–5′ exonucleolytic degradation by polynucleotide phosphorylase [Coburn and Mackie, 1999], and (ii) the nature at the 3′end of the degradation product may reveal some sense of stability of the product, we decided to determine whether the endonuclease generates products with a 3′phosphate or a 3′hydroxy group. We adopted the method described by Schoenberg and co-workers [Chernokalskaya et al., 1997; Schoenberg and Cunningham, 1999] in which digestion with snake venom exonuclease was used to differentiate between products with 3′hydroxyls versus bearing 3′phosphates. Figure 6 shows an experiment where 5′-labeled ^{32}P-CRD RNA was digested with RNase T1 to generate products with 3′phosphates (lanes 3 and 4), S1 nuclease to generate products with 3′ hydroxyls (lanes 6 and 7), and the endonuclease (lanes 9 and 10).

The products of these reactions were either loaded directly onto the gel without further treatment (lanes 3, 6, and 9), or treated with snake venom exonuclease prior to electrophoresis (lanes 4, 7, and 10). The snake venom exonuclease had no effect on most of the degradation products generated by RNase T1 cleavage (compare lane 4 to lane 3). One RNase T1 product (marked with an asterisk in lane 3) was apparently degraded by the exonuclease (compare lane 4 to lane 3) for reasons unknown to us. It is interesting that the exonuclease was inert to the RNA substrate (compare lane 4 to lane 3), suggesting that there may be subpopulation of substrates with 3′ phosphate groups. In contrast, most of the S1 nuclease degradation products (~40–60 nts) were susceptible to degradation by the snake venom exonuclease, as evidence by the disappearance of fragments (compare lane 7 to lane 6). Surprisingly, four degradation products of ~60–83 nts were distinctly generated only upon treatment with the exonuclease (compare lane 7 to lane 6). The ability of snake venom exonuclease to degrade the endonuclease-generated degradation products was investigated next. As shown in lane 9 (Fig. 6), the three typical decay products corresponding to cleavage sites 1720, 1727 and 1730 (shown by arrow) were generated by the endonuclease in addition to the generation of four decay products (shown by asterisks) corresponding to cleavage sites 1742, 1747, 1751 and 1757. The latter four decay products were not taken into consideration when assessing the nature of 3′end RNA product generated by the endonuclease because these decay products were also produced by the exonuclease (compare lane 9 to lane 7). Thus, in evaluating the nature of 3′ end of RNA decay product generated by the endonuclease, we focused on the three typical decay products corresponding to cleavage sites 1720, 1727 and 1730. As shown in lane 10, upon treatment with the snake venom exonuclease, three endonuclease-generated decay products (shown by arrow) showed definitive degradation, suggestive of the presence of 3′ hydroxyl group for 3′–

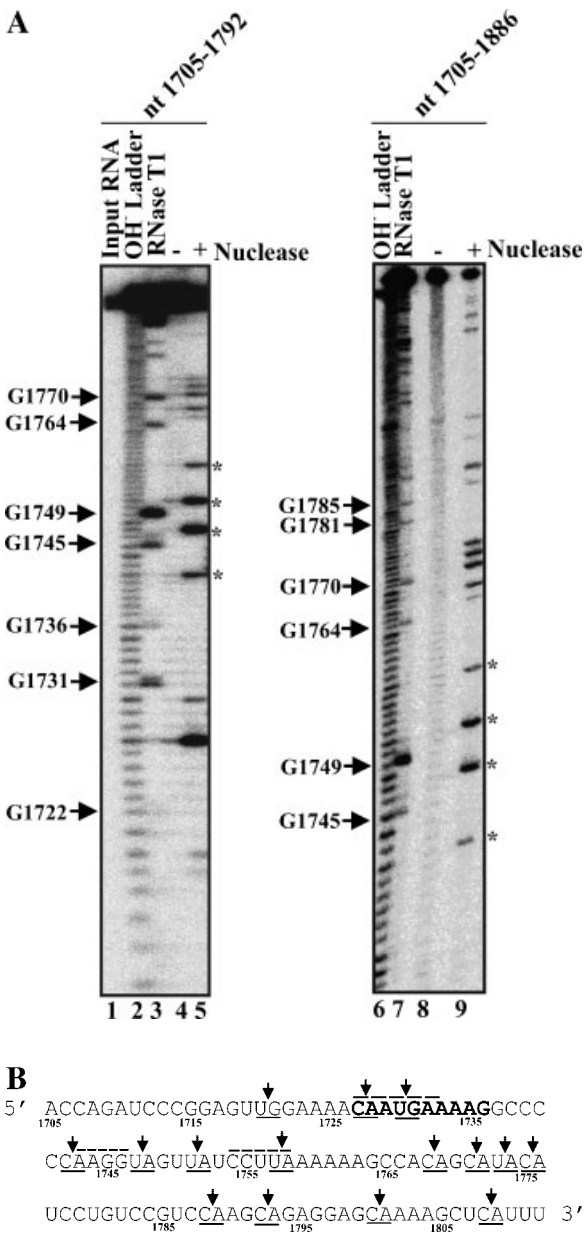

Fig. 3. Determining the exact in vitro cleavage sites on CRD RNA by the partially purified post-heparin Sepharose endonuclease. **A**: CRD RNAs corresponding to nts 1705–1792 (lanes 1–5) and 1705–1886 (lanes 6–9) were $5'^{32}$P-end-labeled and subjected to endonuclease treatment (lanes 5 and 9) as described in Materials and Methods. These radiolabeled RNAs were also subjected to alkaline hydrolysis (lanes 2 and 6) and partial RNase T1 digests (lanes 3 and 7). Lanes 4 and 8 have no addition of enzyme under the standard endonuclease assay. Arrows on the **left** of autoradiogram indicate guanosine (G) cleavage sites generated by RNase T1 and the numbers indicate position of nucleotide sequences. Asterisks indicate the observable identical cleavage products generated by the endonuclease on both RNA substrates. **B**: Sequences on nt 1705–1812 of c-*myc* CRD RNA correspond to the sites identified in (A). Underlined sequences and arrows indicate cleavage sites generated by the endonuclease. Broken lines above sequences indicate cleavage sites generated by a previously described liver endonuclease [Lee et al., 1998]. Bolded sequences at nts 1727–1736 show the previously mapped endonucleolytic cleavage site generated by the liver endonuclease [Lee et al., 1998].

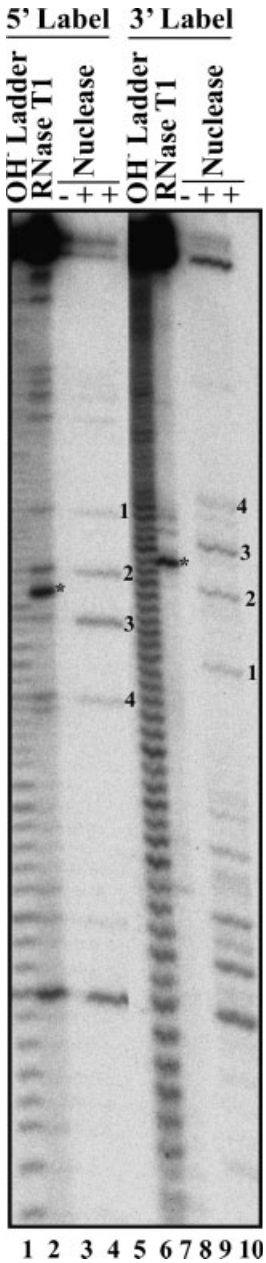

Fig. 4. The partially purified post-heparin Sepharose enzyme is an endonuclease. The 88-nt CRD RNA substrate (nts 1705–1792) was ^{32}P-labeled at its 5′ or its 3′-terminus. Each RNA was incubated under the standard endonuclease conditions for 5 min in the absence (lanes 3 and 8) or presence (lanes 4, 5, 9, and 10) of partially purified endonuclease. The reaction was then stopped and the RNA was harvested. Each RNA was then electrophoresed on a 12% polyarcylamide/7 M urea gel, and the bands were visualized by phosphorImaging. Samples were run along side ^{32}P-labeled CRD RNAs, which had been subjected to alkaline hydrolysis (lanes 1 and 6) or partial RNase T1 digest (lanes 2 and 7). Asterisks indicate the RNase T1 decay product (nt G1749) used as a reference point. Numbers 1–4 indicate the corresponding 5′ and 3′ ends endonucleolytic decay products generated using the 5′ and 3′ labeled RNAs.

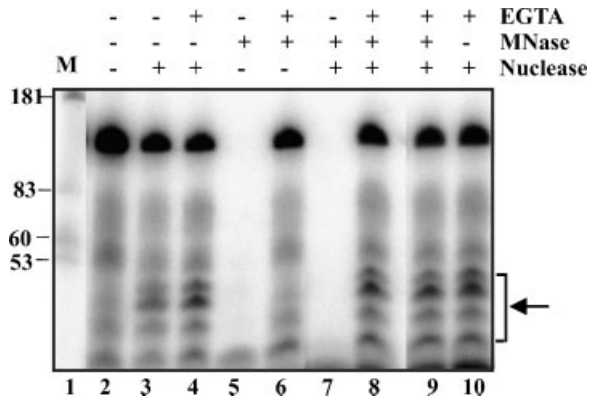

Fig. 5. Evidence that the partially purified post-heparin Sepharose endonuclease is a protein-only enzyme. Three units of pre-treated endonuclease were incubated with 5′^{32}P-end-labeled CRD RNA for 5 min at 37°C in the presence or absence of 5×10^{-2} U of micrococcal nuclease (MNase) and 17 mM EGTA. The endonuclease pre-treatment consisted of incubating the enzyme with or without MNase at 37°C for 5 min prior to addition of EGTA and 5′-labeled CRD RNA. Non-pre-treated endonuclease was used for lanes 2–8 and pre-treated enzymes were used for lanes 9 and 10. Lane 1 is 5′-end-labeled pBR322 ^{32}P-DNA cleaved with *Hae*II. Lane 2, no enzymes or EGTA; lane 3, endonuclease only; lane 4, endonuclease in the presence of EGTA; lane 5, MNase only; lane 6, MNase in the presence of EGTA; lane 7, endonuclease and MNase; lane 8, endonuclease, MNase and EGTA. Lane 9, endonuclease pre-treated with MNase and then with EGTA; lane 10, endonuclease pre-treated with water and then with EGTA. Arrow indicates the endonucleolytic decay products.

5′exonucleolytic degradation by the exonuclease. Two separate experiments were conducted and similar results to Figure 6 were obtained. It is worth noting that under the experimental conditions conducted here, there were incomplete exonucleolytic digestions by the snake venom exonuclease on both S1 nuclease- (compare lane 7 to lane 6) and endonuclease-generated (compare lane 10 to lane 9) decay products.

To support the above findings, we performed another set of experiments using alkaline phosphatase. Internally ^{32}P-labeled 1705–1792 CRD RNA was first digested with the endonuclease followed by treatment with alkaline phophatase. When ran on a 20% high resolution polyacrylamide/urea gel, the mobility shift of endonuclease- and S1 nuclease-generated degradation products were identical upon treatment with phosphatase (data not shown). In contrast, there were greater mobility shifts of RNase T1-generated degradation products of similar sizes (data not shown). This

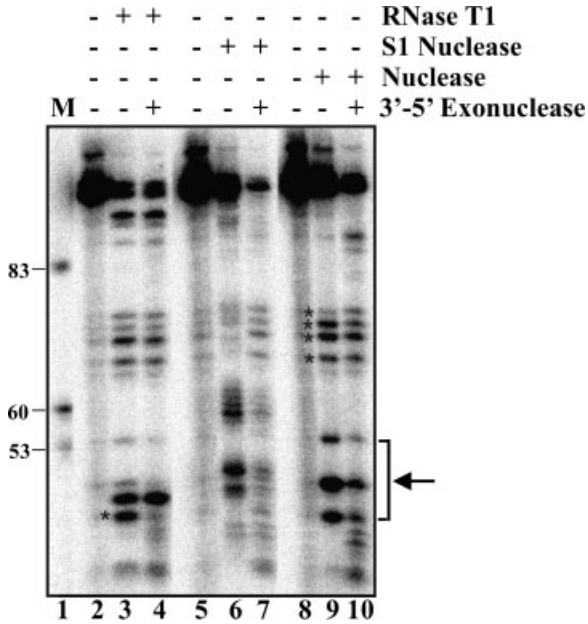

Fig. 6. The partially purified post-heparin Sepharose endonuclease generates products with 3′ hydroxyls. 5′^{32}P-end–labeled CRD RNA was digested with 1 U of RNase T1 (lanes 3 and 4) for 1 min at 37°C, or with 2 U of S1 nuclease (lanes 6 and 7) or 3 U of the endonuclease (lanes 9 and 10) for 5 min at 37°C. The products of these reactions were then incubated for 10 min at 25°C with 3×10^{-2} U of snake venom exonuclease (lanes 4, 7, and 10), and electrophoresed on a 6% polyacrylamide/urea gel. The arrow indicates the position of the three characteristic products generated by the endonuclease. Lane 1 contains the 5′-end-labeled pBR322 ^{32}P-DNA *Hae*II-cleaved marker. Lanes 2, 5, and 8 are the starting substrate transcripts for each type of reactions.

supports the conclusion that the endonuclease generates degradation products with 3′ hydroxyl groups.

The Enzyme Cleaves Single-Stranded RNAs, but not Double-Stranded RNA, DNAs, or DNA–RNA Duplexes

As a first step towards understanding what nucleic acid substrates are preferred by the endonuclease, we challenged the enzyme with single- and double-stranded nucleic acids, which correspond to the CRD sequences of c-*myc* mRNA.

To ensure that the correct substrates were used, we ran each nucleic acid sample on a 10% non-denaturing polyacrylamide gel followed by gel purification of the nucleic acid samples as shown in Figure 7A. The asterisk on each lane shows the desired nucleic acid samples, which were gel purified. Lane 2 shows the 5′-labeled 88-nt 1705–1792 CRD RNA and lane 3 shows the expected smaller fragment of 5′-labeled 88-nt 1705–1792 CRD DNA. Lane 4 shows the intact double-stranded RNA upon hybridization of 5′^{32}P-labeled 1705–1792 CRD RNA with excess antisense 1886–1705 CRD RNA. Also present in lane 4 is the single-stranded 5′^{32}P-labeled 1705–1792 CRD RNA which was either denatured or previously un-hybridized. Lane 5 shows the intact double-stranded DNA upon hybridization of 5′^{32}P-labeled 1705–1792 CRD DNA with excess antisense 1792–1713 CRD oligo. The single-stranded 5′^{32}P-labeled 1705–1792 CRD DNA was also present in small amounts indicating that parts of the double-stranded DNA was denatured or some of the single-stranded DNA was not previously hybridized. Two types of DNA-RNA duplexes were made as shown in lanes 6 and 7. Lane 6 shows the DNA-RNA duplex upon hybridization of 5′^{32}P-labeled 1705–1792 CRD DNA to excess antisense 1886–1705 CRD RNA, and lane 7 shows the RNA-DNA duplex upon hybridization of 5′^{32}P-labeled 1705–1792 CRD RNA to excess antisense 1792–1713 CRD oligo. Traces of single-stranded 5′^{32}P-labeled DNA or RNA were also visible in these lanes for the same reasons described above. Nevertheless, only the desired nucleic acids were gel purified and tested for effects by the endonuclease.

The partially purified endonuclease was challenged with gel purified nucleic acid substrates from Figure 7A and samples were run on a 6% denaturing gel as shown in Figure 7B. Lane 2 and 3 shows the typical three distinct

Fig. 7. The partially purified post-heparin Sepharose endonuclease cleaves single-stranded RNA, but not double-stranded RNA, DNAs, and DNA–RNA duplexes. **A**: CRD RNA and DNA corresponding to nts 1705–1792 of c-*myc* RNA were 5′^{32}P-end-labeled. Double-stranded (ds) nucleic acids were made as described in Materials and Methods. These different combinations of nucleic acids were run on a 10% non-denaturing gel, and bands containing nucleic acids of interest, shown by asterisks, were purified. **B**: Gel purified ^{32}P-labeled single-stranded (ss) RNA, ss DNA, ds DNA, and DNA–RNA duplexes, as indicated, were subjected to the standard endonuclease assay as described in Materials and Methods. Samples were run on a 6% denaturing gel. Marker (M) in lane 1 is 5′-labeled ^{32}P-pBR322 DNA cleaved with *Hae*II. **C**: 5′^{32}P-end-labeled single- (lanes 4 and 5) and double-stranded (lanes 6 and 7) CRD RNAs corresponding to nts 1705–1886 of c-*myc* RNA were subjected to endonuclease assay, and samples were run on a 6% denaturing gel. Lanes 1 and 2 are single-stranded nts 1705–1792 CRD RNA. **D**: The same samples from lanes 4–7 in C were run on 8% non-denaturing gel as indicated.

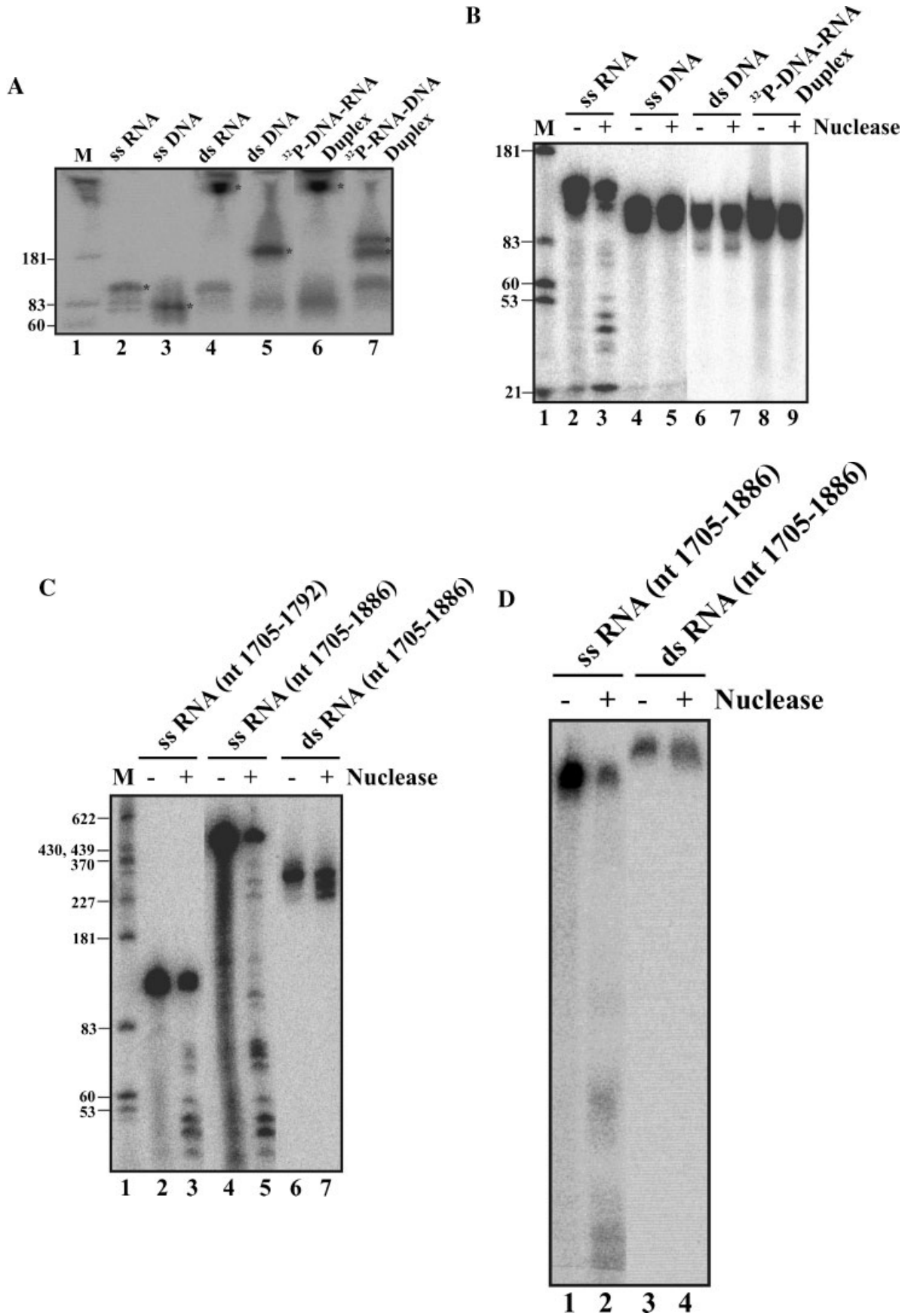
A
M
ss RNA
ss DNA
ds RNA
ds DNA
32P-DNA-RNA Duplex
32P-RNA-DNA Duplex
181
83
60
1 2 3 4 5 6 7
B
ss RNA
ss DNA
ds DNA
32P-DNA-RNA Duplex
M - + - + - + - + Nuclease
181
83
60
53
21
1 2 3 4 5 6 7 8 9
C
ss RNA (nt 1705-1792)
ss RNA (nt 1705-1886)
ds RNA (nt 1705-1886)
M - + - + - + Nuclease
622
430, 439
370
227
181
83
60
53
1 2 3 4 5 6 7
D
ss RNA (nt 1705-1886)
ds RNA (nt 1705-1886)
- + - + Nuclease
1 2 3 4

Fig. 7.

products of ~40–60 nts generated by the endonuclease on 5′^{32}P-labeled 1705–1792 CRD RNA. In contrast, the enzyme had no effect on the single stranded 5′^{32}P-labeled 1705–1792 CRD DNA (lanes 4 and 5) as well as the double-stranded DNA (lanes 5 and 6). Similarly, the endonuclease had no observable effect on DNA-RNA duplexes when either 5′^{32}P-labeled 1705–1792 CRD DNA (lanes 8 and 9) or 5′^{32}P-labeled 1705–1792 CRD RNA (data not shown) was used. These results were further confirmed in experiments where treated samples were run on 10% non-denaturing gel (data not shown). To assess the possible double-stranded RNase activity of the endonuclease, we challenged the enzyme with double-stranded RNA made from complementary single-stranded RNA of identical length. 5′^{32}P-labeled 1705–1886 CRD RNA was hybridized with excess antisense 1886–1705 CRD RNA, and the double-stranded RNA was purified as in Figure 7A. This double-stranded RNA was treated with the endonuclease and samples were run on either 6% denaturing gel (Fig. 7C) or 8% non-denaturing gel (Fig. 7D). It should be mentioned here that the double-stranded RNA appeared to remain intact and have greater mobility (lanes 6 and 7) than its single-stranded counterparts of identical length (lanes 4 and 5) on a denaturing gel (Fig. 7C). This could be attributed to the shape of the double-stranded RNA molecule. On the denaturing gel, slightly faster migrating bands were observed from the double-stranded RNA upon treatment with the enzyme (lanes 6 and 7, Fig. 7C) which is indicative of 'nibbling' at the ends of RNA substrates. On the non-denaturing gel, the double-stranded RNA has slightly lower mobility than its single-stranded counterparts (compare lane 1 to 3, Fig. 7D), and upon treatment with the endonuclease, the double-stranded RNA was only slightly degraded (lanes 3 and 4, Fig. 7D). This is consistent with the results in Figure 7C of the possible 'nibbling' effect at the ends of RNA substrates by the enzyme.

From the above results, we conclude that the endonuclease can cleave both single-stranded RNAs, but neither single- nor double-stranded DNAs, demonstrating that the enzyme is an RNA-specific endonuclease. Furthermore, it does not cleave RNA-DNA duplexes, suggesting that it does not possess RNase H-like activity. The endonuclease does not appear to have any clear endonucleolytic activity on double-stranded RNA.

The Endonuclease Cleaves RNAs Other Than c-*myc* mRNA

Identified vertebrate RNases have been shown to exhibit some degree of specificity. For example, PMR1 from Xenopus has sequence-selectivity for albumin and vitellogenin mRNAs, but not ferritin mRNA [Dompenciel et al., 1995; Cunningham et al., 2001]. A previously described liver endonuclease preferentially cleaves a specific region in c-*myc* CRD when challenged with either of 1705–1792 or 1705–1886 CRD [Lee et al., 1998], but no specific degradation by the enzyme was seen with nts 1–217 from 5′-UTR of c-*myc* mRNA [Lee et al., 1998]. The issue of substrate selectivity by the endonuclease described in this paper was addressed by the experiment described in Figure 8. The partially purified endonuclease was challenged with four deproteinized 5′-^{32}P-RNA substrates as follows: c-*myc* 5′-CRD RNA (nts 1705–1792), β-globin RNA (nts 50–169), MDR1 RNA (nts 745–922), and nts 1–270 from the c-*myc* mRNA. As shown, all RNAs tested were cleaved by the endonuclease to generate specific fragments. Judging from the identical cleavage sites generated by the endonuclease on nts 1705–1792 and 1705–1886 of c-*myc* RNA (Fig. 3A), and the specific fragments generated by the enzyme on other RNAs, we conclude that the endonuclease is not substrate-specific but rather a sequence-selective RNA endonuclease.

Sensitivity to Temperature and Requirements for Mg^{2+}

We have shown that a previously purified 39 kDa liver endonuclease was completely inactivated when incubated at 50°C for 5 min [Lee et al., 1998]. To test to see if the enzyme described in this paper is distinct, we subjected the enzyme to several temperatures and then examined their nucleolytic activity. Our results showed that the endonuclease activity remained active up to 60°C and was only completely inactivated at 70°C (data not shown). The previously described liver endonuclease has been shown to absolutely require Mg^{2+} for its endonucleolytic activity [Lee et al., 1998]. The requirement for Mg^{2+} by the currently described endonuclease was tested, and our results showed that the enzyme remained active in the absence of Mg^{2+} (data not shown).

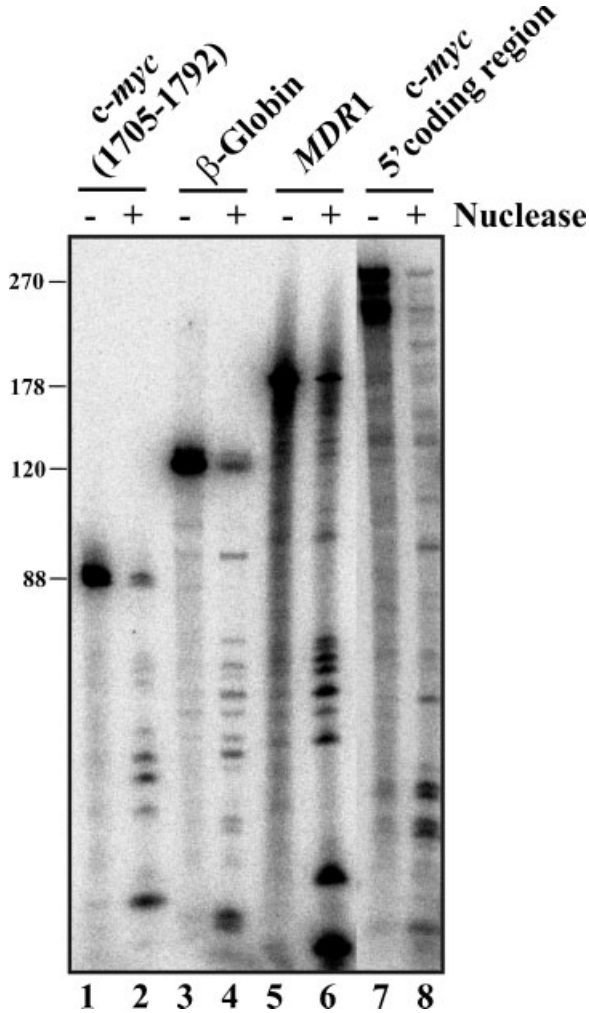

Fig. 8. Effect of the partially purified post-heparin Sepharose endonuclease on various in vitro transcribed RNAs. One unit of partially purified endonuclease was incubated for 5 min at 37°C with the following deproteinized, 5′-end-labeled ^{32}P-RNAs: lane 1 and 2, 5′-CRD (c-*myc* nts 1705–1792); lanes 3 and 4, β-globin (nts 50–169); lanes 5 and 6, MDR1 (nts 745–922); and lanes 7 and 8, 5′coding region of c-*myc* RNA (nts 1–270). Numbers on the left indicate sizes (nt) of the ^{32}P-RNA substrates.

Thus, we concluded that the two liver endonucleases are distinct in their temperature sensitivity and requirements for Mg^{2+}.

DISCUSSION

This study describes the biochemical characteristics and partial purification of a second mammalian polysome-associated endonuclease that is capable of degrading c-*myc* CRD RNA in vitro. This study was initiated based on the following rationale: (1) There was evidence for the role of CRD in degradation and/or regulation of c-*myc* mRNA in cells. (a) c-*myc* mRNA was still unstable when 5′- and 3′-UTRs are deleted, indicating that the c-*myc* mRNA coding region contains an instability determinant [Jones and Cole, 1987; Bonnieu et al., 1990]. (b) CRD is required for the post-transcriptional down-regulation of c-*myc* mRNA during differentiation of muscle cells [Wisdom and Lee, 1991; Yielding and Lee, 1997]. (c) The coding region of c-*myc* mRNA is required for the post-transcriptional downregulation of c-*myc* mRNA levels during liver regeneration [Jones and Cole, 1987; Pistoi et al., 1996; Steer, 1996]. (d) The CRD is an instability element in cells independent of other regions of c-*myc* mRNA. When CRD is inserted into the coding region of stable globin mRNA to generate globin-MYC-globin mRNA, the new fusion mRNA became unstable in cells [Herrick and Ross, 1994]. (e) c-*myc* mRNA decay intermediates which correspond to the CRD have been identified in cells [Hanson and Schoenberg, 2001], supporting the notion that in vivo degradation of c-*myc* mRNA involves endonucleolytic cleavage. (2) While we know the identity of key endonucleases involved in the degradation and processing of tRNAs and rRNAs, very little is known about endonucleases that degrade mRNAs in mammalian cells. (3) As outlined in the Introduction, there is evidence for endonuclease-mediated mRNA decay in vertebrates, but yet only few have been described. (4) Since mRNA-degrading enzymes must play critical roles in regulating and controlling mRNA turnover and abundance, it is imperative that these groups of enzymes be identified and studied in order to fully understand how mammalian mRNAs are degraded, and to understand the overall significance of mRNA degradation in the biology of gene expression. (5) Significant role of endonuclease has been physiologically demonstrated in vertebrates as evidenced from the RNA interference system.

Five major protein bands of ~10–35 kDa copurified with the endonuclease activity in the final chromatography column heparin-sepharose (Fig. 1C). Two further findings support the proposal that one or a combination of these proteins contribute to the endonuclease activity. (i) The endonuclease activity migrates in the ~34 kDa range in a glycerol gradient (Fig. 2A). (ii) The most prominent endonuclease activity migrates at ~35 kDa and a weaker endonuclease activity at ~13 kDa by gel filtration

(Fig. 2B). Like other vertebrate endonucleases [Dompenciel et al., 1995; Lee et al., 1998; Provost et al., 2002; Rodgers et al., 2002], the endonuclease may form complexes with other proteins or multimerizes as we have observed its activity in the range of ~45–66 kDa in a glycerol gradient when crude ribosomal salt wash was used (data not shown). Treatment of the partially purified endonuclease with micrococcal nuclease had no effect, suggesting that unlike RNase P [Gopalan et al., 2002] and MRP [Xiao et al., 2002], an RNA component is not required for its activity. Experiments using snake venom exonuclease demonstrated that the endonuclease generates RNA decay products with 3′ hydroxyl groups, suggesting that its decay products are likely to be less stable in cells. Our studies provide strong evidence that the endonuclease is an RNA-specific endonuclease. It cleaves single-stranded RNA, but not double-stranded RNA, DNAs or DNA–RNA duplexes. It is important to point out that although the endonuclease degrades single-stranded RNA and has no effect on double-stranded RNA, it is still not known if it cleaves at the single- or double-stranded form of RNA or both. The secondary structure of CRD RNA would have to be determined to clarify this.

Several biochemical studies confirmed that the endonuclease described in this article and the previously purified liver endonuclease [Lee et al., 1998] are indeed distinct enzymes. (i) While the previously described enzyme is completely inactivated at 50°C [Lee et al., 1998], the present endonuclease remained active even at 60°C. (ii) The previously described enzyme absolutely requires Mg^{2+} for its activity [Lee et al., 1998] but the present endonuclease is Mg^{2+}-independent. (iii) The previously described enzyme is sensitive to vanadyl ribonucleoside complex [Lee et al., 1998] while the present endonuclease is insensitive to the RNase inhibitor (Lee, unpublished observation). (iv) The previously described enzyme has relative specificity for c-*myc* CRD RNA [Lee et al., 1998] but the present endonuclease cleaves RNAs other than c-*myc* CRD RNA (Fig. 8). (v) Cleavage sites generated by both endonucleases do not overlap. For instance, AAGG at nts 1743–1745 were specifically cleaved by the previously described enzyme (Fig. 3B), while UA (nts 1747 and 1751), UG (nt 1720), and CA (nts 1742 and 1768) were specifically cleaved by the present enzyme (Fig. 3). Using the PCR-based poly(A)-tailing method, the major cleavage site generated by the previously described enzyme was mapped to only the 10-nt segment between nts 1727 and 1736 with the sequence 5′-CAAUGAAAAG-3′ [Lee et al., 1998]. It is possible that the other cleavage sites identified in this study were overlooked by the PCR-based poly(A)-tailing method since only 8 positive clones were sequenced [Lee et al., 1998]. Consistent with this finding, mapped cleavage sites generated by the previously described enzyme include CAAUGAA at nts 1727–1732, and mapped cleavage sites by the present endonuclease include the dinucleotide CA at nt 1727 (Fig. 3B). It is worth noting that the major cleavage site CA at nt 1727 was generated by both endonucleases, and this site corresponds precisely to a c-*myc* mRNA degradation intermediate identified in murine erythroleukemia cells using ligation-mediated PCR method [Hanson and Schoenberg, 2001]. This supports the notion that in vivo degradation of c-*myc* mRNA involves endonucleolytic cleavage and highlights the possible significance of both endonucleases described here in the post-transcriptional control of c-*myc* mRNA in cells. Studies are currently underway to determine the secondary structure of the CRD in vitro and in vivo, which will further reveal the nature of cleavage properties as well as the substrates of the endonucleases.

Unlike the previously described enzyme, the present endonuclease does not appear to possess properties such as Mg^{2+}-dependence and sensitivity to vanadyl ribonucleoside complex which are inherent to the identified c-*myc* endonuclease [Lee et al., 1998]. Such findings revealed that not all polysomal endonucleases will have properties resembling c-*myc* endonuclease, which further underscores the significance of the previously described endonuclease for the degradation of c-*myc* mRNA. Supporting this notion is the observation that this enzyme has remarkable relative specificity for c-*myc* CRD [Lee et al., 1998], whereas the present endonuclease does not exhibit any degree of specificity for c-*myc* CRD (Fig. 8). Despite such differences in their in vitro properties, it will still be important to determine whether both enzymes can degrade c-*myc* mRNA in cells, especially when the shielding CRD RNA-binding protein, called CRD-BP [Bernstein et al., 1992; Prokipcak et al., 1994], is present.

Some vertebrate RNases have been shown to be relatively specific. For example, PMR1 that preferentially cleaves RNA within single-stranded consensus pentamer APyrUGA, has a relative specificity for albumin and vitellogenin mRNA [Chernokalskaya et al., 1998], and a previously described liver endonuclease has some preference for the CRD of c-*myc* mRNA [Lee et al., 1998]. For many other RNases [Claverie-Martin et al., 1997; Van Dijk et al., 1998; Tourriere et al., 2001; Rodgers et al., 2002], the issue of substrate-specificity has not been addressed. In this study, we showed that the endonuclease has cleavage preference for some UA, UG, and CA dinucleotides of c-*myc* CRD. It is likely that both the secondary structure of the CRD RNA and the orientation of the endonuclease to the RNA are the major determining factors for its cleavage preferences. Further detailed investigations into the endonuclease RNA sequence and structural recognition for cleavage will be required. Given that the enzyme has preference for these dinucleotides, it will not be surprising if it can also degrade different RNA substrates. Our studies, in fact, showed that the enzyme also cleaves *MDR*1 and β-globin at UA and UG dinucleotides (unpublished observations).

At first glance on the effect of the endonuclease on CRD RNA, it does appear that the enzyme activity is the result of a non-specific RNase A or RNase A-like activity. However, three observations proved otherwise: (i) While RNase A generates products with 3′ phosphate groups, the endonuclease generates products with 3′ hydroxyl groups (Fig. 6). (ii) At concentrations (1–20 U) which completely inhibited RNase A, RNasin had no effect on the endonuclease activity (unpublished observations). (iii) Both RNase A and the endonuclease cleaved *MDR*1 and β-globin RNA substrates at distinct sites in vitro (Lee, unpublished observations).

We conclude that the enzyme described in this article is a novel mammalian endonuclease with properties that further distinguish it from other previously reported vertebrate endonucleases, including the previously described liver endonuclease [Lee et al., 1998]. These include a ~60-kDa *Xenopus* liver polysomal endonuclease PMR1 that preferentially degrades albumin mRNA [Dompenciel et al., 1995; Chernokalskaya et al., 1998], a ~120-kDa endonuclease from *Xenopus* and *Drosophilia* cells that preferentially attacks maternal homeobox mRNAs [Brown et al., 1993], a ~68-kDa endonuclease from T-cells that preferentially degrades interleukin-2 mRNA in vitro [Hua et al., 1993], a 13.3-kDa human endonuclease [Wennborg et al., 1995] and a ~65-kDa enzyme [Claverie-Martin et al., 1997] that share several properties with *E. coli* enzyme RNase E, a ~40-kDa endonuclease ErEN that is enriched in erythroid cells and preferentially attacks 3′UTR of α-globin mRNA [Wang and Kiledjian, 2000; Rodgers et al., 2002], a 218-kDa human endonuclease Dicer that possesses double-stranded RNase activity and is involved in RNA silencing [Provost et al., 2002], a ~52 kDa protein known as G3BP that preferentially cleaves CA dinucleotides at 3′UTR of c-*myc* mRNA [Tourriere et al., 2001], and a ~26 kDa hepatic endonuclease that cleaves hepatitis B viral RNA [Heise et al., 2001]. By having partially purified the endonuclease and identified the five major bands that co-purified with its activity, it should now be possible to obtain the identity of these proteins. Experiments using the recombinant form of these proteins should definitively confirm whether the endonuclease activity is indeed contributed by one or several of these proteins.

ACKNOWLEDGMENTS

C.H.L. is a Research Scientist of the National Cancer Institute of Canada supported with funds provided by the Canadian Cancer Society. E.D. was supported by a BC Cancer Summer Studentship provided by the Canadian Breast Cancer Foundation.

REFERENCES

Bernstein PL, Herrick DJ, Prokipcak RD, Ross J. 1992. Control of c-*myc* mRNA half-life in vitro by a protein capable of binding to a coding region determinant. Genes Dev 6:642–654.

Binder R, Hwang SP, Basilion JP, Koeller DM, Klausner RD, Harford JB. 1994. Degradation of apolipoprotein II mRNA occurs via endonucleolytic cleavage at 5′-AAU-3′/5′-UAA-3′ elements in single-stranded loop domains of the 3′-noncoding region. EMBO J 13:1969–1980.

Bonnieu A, Roux P, Marty L, Jeanteur P, Piechaczyk M. 1990. AUUUA motifs are dispensable for rapid degradation of the mouse c-*myc* RNA. Oncogene 5:1585–1588.

Brewer G. 1999. Evidence for a 3′-5′ decay pathway for c-*myc* mRNA in mammalian cells. J Biol Chem 274:16174–16179.

Brewer G. 2000. Regulation of c-*myc* mRNA decay in vitro by a phorbol ester-inducible, ribosome-associated component in differentiating megakaryoblasts. J Biol Chem 275:33336–33345.

Brewer G. 2002. Messenger RNA decay during aging and development. Ageing Res Rev 1:607–625.

Brown BD, Zipkin ID, Harland RM. 1993. Endonucleolytic cleavage of a maternal homeo box mRNA in *Xenopus* oocytes. Genes Dev 7:1620–1631.

Carmell MA, Hannon GJ. 2004. RNase III enzymes and the initiation of gene silencing. Nat Struct Mol Biol 11:214–218.

Chernokalskaya E, Dompenciel RE, Schoenberg DR. 1997. Cleavage properties of an estrogen-regulated polysomal ribonuclease involved in the destabilization of albumin mRNA. Nucleic Acids Res 25:735–742.

Chernokalskaya E, Dubell AN, Cunningham KS, Hanson MN, Dompenciel RE, Schoenberg DR. 1998. A polysomal ribonuclease involved in the destabilization of albumin mRNA is a novel member of the peroxidase gene family. RNA 4:1537–1548.

Claverie-Martin F, Wang M, Cohen SN. 1997. ARD-1 cDNA from human cells encodes a site specific single-stranded endoribonuclease that functionally resembles *Escherichia coli* RNase E. J Biol Chem 272:13823–13828.

Coburn GA, Mackie GA. 1999. Degradation of mRNA in *Escherichia Coli*: An old problem with some new twist. Prog Nucleic Acid Res 62:55–108.

Cunningham KS, Hanson MN, Schoenberg DR. 2001. Cleavage properties of an estrogen-regulated polysomal ribonuclease involved in the destabilization of albumin mRNA. Nucleic Acids Res 29:1156–1162.

Dodson RE, Shapiro DJ. 2002. Regulation of pathways of mRNA destabilization and stabilization. Prog Nucleic Acid Res 72:129–164.

Dompenciel RE, Garnepudi VR, Schoenberg DR. 1995. Purification and characterization of an estrogen-regulated *Xenopus* liver polysomal nuclease involved in the selective destabilization of albumin mRNA. J Biol Chem 270:6108–6118.

Fan J, Yang X, Wang W, Wood WH III, Becker KG, Gorospe M. 2002. Global analysis of stress-regulated mRNA turnover by using cDNA arrays. Proc Natl Acad Sci USA 99:10611–10616.

Gatfield D, Izaurralde E. 2004. Nonsense-mediated messenger RNA decay is initiated by endonucleolytic cleavage in *Drosophila*. Nature 429:575–578.

Gazzani S, Lawrenson T, Woodward C, Headon D, Sablowski R. 2004. A link between mRNA turnover and RNA interference in *Arabidopsis*. Science 306:1046–1048.

Gopalan V, Vioque A, Altman S. 2002. RNase P: Variations and uses. J Biol Chem 277:6759–6762.

Hanson MN, Schoenberg DR. 2001. Identification of in vivo mRNA decay intermediates corresponding to sites of in vitro cleavage by polysomal ribonuclease 1. J Biol Chem 276:12331–12337.

Heise T, Guidotti LG, Chisari FV. 2001. Characterization of nuclear RNases that cleave hepatitis B virus RNA near the La protein binding site. J Virol 75: 6874–6883.

Herrick DJ, Ross J. 1994. The half-life of c-*myc* mRNA in growing and serum-stimulated cells: Influence of the coding and 3′ untranslated regions and role of ribosome translocation. Mol Cell Biol 14:2119–2128.

Hua J, Garner R, Paetkau V. 1993. An RNasin-resistant ribonuclease selective for interleukin 2 mRNA. Nucleic Acids Res 21:155–162.

Ioannidis P, Havredaki M, Courtis N, Trangas T. 1996. In vivo generation of 3′ and 5′truncated species in the process of c-*myc* mRNA decay. Nucleic Acids Res 24:4969–4977.

Jones TR, Cole MD. 1987. Rapid cytoplasmic turnover of c-*myc* mRNA: Requirement of the 3′ untranslated sequences. Mol Cell Biol 7:4513–4521.

Lee CH, Leeds P, Ross J. 1998. Purification and characterization of a polysome-associated endoribonuclease that degrades c-*myc* mRNA in vitro. J Biol Chem 273:25261–25271.

Morello D, Fitzgerald MJ, Babinet C, Fausto N. 1990. c-*myc*, c-fos, and c-jun regulation in the regenerating livers of normal and H-2K/c-myc transgenic mice. Mol Cell Biol 10:3185–3193.

Parker R, Song H. 2004. The enzymes and control of eukaryotic mRNA turnover. Nature Struct Mol Biol 11:121–127.

Pistoi S, Roland J, Babinet C, Morello D. 1996. Exon 2-mediated c-*myc* mRNA decay in vivo is independent of its translation. Mol Cell Biol 16:5107–5116.

Prokipcak RD, Herrick DJ, Ross J. 1994. Purification and properties of a protein that binds to the C-terminal coding region of c-*myc* mRNA. J Biol Chem 269:9261–9269.

Provost P, Dishart D, Doucet J, Frendewey D, Samuelsson B, Radmark O. 2002. Ribonuclease activity and RNA binding of recombinant human Dicer. EMBO J 21:5864–5874.

Raghavan A, Ogilvie RL, Reilly C, Abelson ML, Raghavan S, Vasdewani J, Krathwohl M, Bohjanen PR. 2002. Genome-wide analysis of mRNA decay in resting and activated primary human T lymphocytes. Nucleic Acid Res 30:5529–5538.

Rodgers ND, Wang Z, Kiledjian M. 2002. Characterization and purification of a mammalian endoribonuclease specific for the α-globin mRNA. J Biol Chem 277:2597–2604.

Ross J. 1995. mRNA stability in mammalian cells. Microbiol Rev 59:423–450.

Schoenberg DR, Cunningham KS. 1999. Characterization of mRNA endonucleases. Methods 17:60–73.

Steer CJ. 1996. Posttranscriptional regulation of gene expression in liver regeneration: Role of mRNA stability. FASEB J 10:559–573.

Stevens A, Wang Y, Bremer K, Zhang J, Hoepfner R, Antoniou M, Schoenberg DR, Maquat LE. 2002. β-globin mRNA decay in erythroid cells: UG site-preferred endonucleolytic cleavage that is augmented by a premature termination codon. Proc Natl Acad Sci USA 99:12741–12746.

Swartwout SG, Kinniburgh AJ. 1989. c-*myc* RNA degradation in growing and differentiating cells: Possible alternate pathways. Mol Cell Biol 9:288–295.

Tharun S, Parker R. 1997. Mechanisms of mRNA turnover in eukaryotic cells. In: Harford J, Morris DR, editors. mRNA metabolism and post-transcriptional gene regulation. New York: Wiley-Liss. pp 181–200.

Tharun S, Sirdeshmukh R. 1995. Specific endonucleolytic cleavages of mouse albumin mRNA and their modulation during liver development. Nucleic Acids Res 2:641–646.

Tourriere H, Gallouzi I-E, Chebli K, Capony JP, Mouaikel J, Van der Geer P, Tazi J. 2001. RasGAP-associated endoribonuclease G3BP: Selective RNA degradation and phosphorylation-dependent localization. Mol Cell Biol 21:7747–7760.

Van Dijk EL, Sussenbach JS, Holythuizen PE. 1998. Identification of RNA sequences and structures involved in site-specific cleavage of IGF-II mRNAs. RNA 4:1623–1635.

Wang Z, Kiledjian M. 2000. Identification of an erythroid-enriched endonuclease activity involved in specific mRNA cleavage. EMBO J 19:295–305.

Wennborg A, Sohlberg B, Angerer D, Klein G, Von Gabain A. 1995. A human RNase E-like activity that cleaves RNA sequences involved in mRNA stability control. Proc Natl Acad Sci USA 92:7322–7326.

Wisdom R, Lee W. 1991. The protein coding region of c-*myc* mRNA contains a sequence that specifies rapid mRNA turnover and induction by protein synthesis inhibitor. Genes Dev 5:232–243.

Xiao S, Scott F, Fierke CA, Engelke DR. 2002. Eukaryotic ribonuclease P: A plurality of ribonucleoprotein enzymes. Annu Rev Biochem 71:165–189.

Yielding NM, Lee WMF. 1997. Coding elements in exons 2 and 3 target c-*myc* mRNA downregulation during myogenic differentiation. Mol Cell Biol 17: 2698–2707.